Carbohydrate Polymers 84 (2011) 1182–1191

Contents lists available at ScienceDirect

Carbohydrate Polymers

journal homepage: www.elsevier.com/locate/carbpol

Characterization of hyaluronate lyase from *Streptococcus pyogenes* bacteriophage H4489A

Nermeen S. El-Safory[a], Guan-Chiun Lee[b], Cheng-Kang Lee[a,*]

[a] Department of Chemical Engineering, National Taiwan University of Science and Technology, 43 Keelung Rd. Sec. 4, Taipei 106-07, Taiwan, ROC
[b] Department of Life Science, National Taiwan Normal University, Taipei, Taiwan, ROC

ARTICLE INFO

Article history:
Received 23 November 2010
Received in revised form 4 January 2011
Accepted 11 January 2011
Available online 18 January 2011

Keywords:
Hyaluronate lyase
Purification
Characterization
Kinetics
Structure

ABSTRACT

Hyaluronate (HA) lyase of *Streptococcus pyogenes* bacteriophage H4489A, was expressed in *Escherichia coli*, purified, and characterized. The purified homogeneous preparation of HA lyase had a molecular mass of 40 kDa. The optimum enzymatic activity was achieved at pH ~ 5.5 and 37 °C, and the enzyme was stable at pH profile from 4 to 7 and temperature range from 25 to 45 °C. The enzymatic activity was vaguely enhanced by Mg^{2+}, slightly inhibited by Ca^{2+}, triton X-100, and Tween 80, strongly inhibited by Zn^{2+}, and completely inhibited by Cu^{2+}, Ni^{2+}, Co^{2+} and sodium dodecyl sulfate. Kinetic measurements give Michaelis constant of 0.44 mg/ml, maximal velocity of 0.20 μmol ml^{-1} min^{-1}, and showed that bacteriophage HA lyase degraded the HA efficiently. Light scattering dynamic measurements determined the denaturation temperate of HA lyase of about 46 °C. Circular dichromism and UV–visible absorption spectroscopy estimated the changes in secondary structure of native and denatureated HA lyase.

1. Introduction

Hyaluronate (HA) lyases (EC 4.2.2.1, hyaluronidases), degrades HA by endolytically cleaving N-acetylglucosamidic bonds to produce unsaturated oligosaccharides with a Δ-4,5-uronate residue at nonreducing termini (Yamagata, Saito, Habuchi, & Suzuki, 1968). HA lyases are generally produced by many different genera of bacteria, including several pathogens of *Streptococci* groups such as *S. agalactiae*, *S. pyogenes*, *S. pneumoniae*, *S. intermedius*, *S. consellatus*, *S. dysgalactiae*, *S. uberis* and *S. zooepidemicus* (Berry et al., 1994; Calvinho, Almeida, & Oliver, 1998; Gunther, Ozegowski, & Kohler, 1996; Guo, Liu, Zhu, Su, & Ling, 2009; Homer, Denbow, Whiley, & Beighton, 1993; Hynes & Walton, 2000; Schaufuss, Sting, Schaeg, & Blobel, 1989). It can also be produced from the bacteriophage of *S. pyogenes* with wide substrate specificity (Hynes & Walton, 2000). The degradation of polymeric HA and other glycosaminoglycans by HA lyases plays an essential roles in many biological processes (El-Safory, Fazary, & Lee, 2010; Kostyukova, Volkova, Ivanova, & Kvetnaya, 1995; Linhardt, Galliher, & Cooney, 1986; Lui & Nizet, 2004; Polissi et al., 1998; Starrl & Engleberg, 2006).

It was known that, the HA lyase isolated from group A *Streptococci* or group B *Streptococci* shows a significant activities towards chondroitin and/or chondroitin 4/6-sulfate, besides cleaving HA (El-Safory et al., 2010). Among the HA lyases known, the most considered ones are those secreted by strains of group B *Streptococci* with a broad substrate specificity such as HA and certain chondroitin sulfates (CS) (Lui & Nizet, 2004). Also, the pathogens of group A *Streptococci* produces a number of different hyaluronidases (Beres et al., 2002; Ferretti et al., 2001; Hynes, Dixon, Walton, & Aridgides, 2000; Hynes & Ferretti, 1989; Hynes, Hancock, & Ferretti, 1995; Smoot et al., 2002). Unlike most bacterial hyaluronidases, which act nonspecifically on both HA and CS, the phage-specific hyaluronidases from *S. pyogenes* (Hynes et al., 1995; Marciel, Kapur, & Musser, 1997) and *Streptococcus equi* (Harrington, Sutcliffe, & Chanter, 2002) were specifically cleaving HA (Baker, Dong, & Pritchard, 2002; Benchetrit, Gray, Edstrom, & Wannamaker, 1978; Hynes et al., 2000, 1995; Hynes & Ferretti, 1989; Niemann, Birch-Andersen, Kjems, Mansa, & Stirm, 1976).

The HA lyase genes found in the bacteriophage genomes showed a high degree of similarity to each other with one major difference being the deletion (or addition) of a 102-bp fragment that consists of a region that encodes a collagen-like motif, Gly-X-Y repeating units (Hynes et al., 1995; Kjems, 1958; Maxted, 1952). Due to this difference, they have been grouped into two types; the HylP1-type, which contains a collagen-like repeat sequence and the HylP2-type, which lacks this repeat sequence. Based on the presence of collagen-like domain, it has been speculated that the HylP-type proteins might be stabilized as a triple helical structure (Stern & Stern, 1992). Recent studies on the sequence of the phage-specific hyaluronidases suggested a different molecular structure and architecture of the phage HA lyase belonging to CAZy polysac-

* Corresponding author. Tel.: +886 2 2737 6629; fax: +886 2 2737 6644.
E-mail addresses: nermeen.elsafory@gmail.com (N.S. El-Safory), cklee@mail.ntust.edu.tw (C.-K. Lee).

0144-8617/$ – see front matter © 2011 Elsevier Ltd. All rights reserved.
doi:10.1016/j.carbpol.2011.01.019

charide lyase family 16, from those of *Streptococcal* ones which belong to a different polysaccharide lyase family 8 (Smith et al., 2005). Also, the three-dimensional structure of *S. pyogenes* HA lyase (HylP1) revealed an unusual triple-stranded β-helical structure (Smith et al., 2005). Moreover, the X-ray crystallography of HylP2-type hyaluronidases found in bacteriophage *S. pyogenes* 10403 have been recently solved (Mishra et al., 2009).

One of the main directions of investigation in applied enzyme engineering is to study the stability and activity of enzyme molecule against various conditions such as pH, temperature, metal ions, denaturants, and surfactants (Mukherjee & Banerjee, 2006, 2007). In this study, hyaluronate (HA) lyase of *S. pyogenes* bacteriophage H4489A was expressed in *E. coli* and purified using immobilized affinity, and ion exchange chromatography techniques. Extraction and all purification steps were checked by SDS-PAGE electrophoresis. Also, the enzyme purity and activity was detected by the means of zymography. Protein content and activity of the enzyme were measured in all steps of extraction and purification. The activities were estimated by colorimetric and turbidity assays, and the effects of pH, temperature, metal ions (Ca (II), Ni (II), Zn (II), Co (II), Cu (II), and Mg (II)), and surfactants (triton X-100, Tween 80) on the activity of the purified phage HA lyase were studied. Time/HA substrate-independent kinetic measurements were evaluated and their associated enzymatic kinetic parameters; Michaelis constant (K_m), and maximal velocity (V_{max}) were calculated and evaluated. Light scattering dynamic measurements were employed to estimate the HA lyase thermal denaturation, and thermal aggregation. In addition, far UV - circular dichromism, and UV–visible absorption spectroscopy techniques were used to characterize the denaturation effects of both guanidinium hydrochloride (GdnHCl) and urea in HA lyase by following the changes in the HA lyase secondary structure. This characterization data provided an important basis for the exploitation of HA lyases.

2. Experimental

2.1. Materials

Plasmid pSF49, containing the HA lyase hylP gene of *S. pyogenes* bacteriophage H4489A, was kindly supplied by Dr Wayne L. Hynes (Department of Biological Science, Old Dominion University, Norfolk, VA). *Pfu* DNA polymerase, T4 Ligation enzymes and, dNTPs were purchased from New England Biolabs, UK. DNA makers and plasmid vector pET30b were purchased from Novagen, UK. Polymerase chain reaction (PCR) purification and gel extraction kits were purchased from Qiagen, USA. Plasmid miniprep kit was purchased from Viogene, Taiwan. *E. coli* strain DH5α, BL21 (DE3) and DNA markers bring from Eastern Biotech. A protein marker was purchased from Fermentas. Isopropyl-β-D-thiogalactopyranoside (IPTG) and kanamycin were purchased from Sigma, USA. Sodium hyaluronate was obtained from Fine Chemical Division of Q.P. Co. (Tokyo, Japan). All other chemicals such as metal ions, detergents, and solvents used in this study are analytic grade and were purchased from Acros, Merck and Sigma companies.

2.2. Phage HA lyase vector construct

An open reading frame fragment of *S. pyogenes* bacteriophage H4489A encoding hylP (GenBank accession number M19348.1) was amplified from plasmid pSF49 using a forward primer containing an *NdeI* site (5′-CCGCATATGACTGAA AATATACCATTAAGAGTC-3′) and a reverse primer containing a *NotI* site (5′-CCGGCGGCCGCTC AATGATGATGATGATGATGTTTTTTTAGTATGAGTTTTTTTAA-3′) by PCR. The amplified hylP gene fragment was purified by PCR extraction Kit. After digestion with *NdeI* and *NotI* using standard procedures, the hylP gene fragment was ligated into a pET30b vector. The product (pET30b-hylp) was transformed into *E. coli* DH5α and selected on Luria–Bertani (LB) medium plates containing 50 μg/mL kanamycin. DNA sequencing confirmed the homogeneity of the sequence. The plasmid pET30b-*hylp* was then transformed into the expression host, *E. coli* BL21 (DE3) for HA lyase protein production.

2.3. Expression and purification of HA lyase

The recombinant strain *E. coli* BL21 (DE3)/pET30b-hylp was grown overnight at 37 °C in LB medium containing 50 μg/mL kanamycin. Overnight cultures were diluted (1:100) by fresh LB kanamycin media and incubated at 37 °C with 200 rpm shaking. HA lyase expression was induced by adding IPTG to give a final concentration of 1 mM when the culture absorbance at 600 nm reached 0.8. After 3 h induction at 30 °C, the cells were harvested by centrifugation (11,000 rpm). Then, the cells pellets were washed twice using 0.1 M phosphate buffer pH 7.4, and re-suspended in 20 mM phosphate, 500 mM NaCl buffer pH 7.4, contain 20 mM imidazole, 1 mg/ml lysosyme, 0.1% triton X-100 and 1 mM PMSF and keep in ice for 30 min before sonication. The sample was in an ice-bath, and sonication was carried out in short bursts in order to avoid overheating the mixture ultrasonic cell disruptor (Microson model XL200). The lysate was centrifuged at 11,000 rpm for 20 min at 4 °C. The expression level was analyzed by gel analysis software after SDS–PAGE analysis. For purification, the supernatant of the cell lyses was loaded onto Histrap FF column for immobilized metal affinity chromatography (IMAC) purification. The target enzyme was eluted by stepwise gradient elution of imidazole from 20 to 500 mM use AKTA Chromtography System (GE Healthcare, USA). The active eluted enzyme fractions were pooled and subjected to dialysis against 50 mM sodium acetate buffer pH 5.5 and then loaded into HiTrap SP FF column. The enzyme was eluted by stepwise gradient elution use the sodium acetate buffer pH 5.5 (0–1 M) NaCl, using AKTA Chromatography System. After that, the active enzyme was dialysis against 50 mM acetate buffer pH 5.5 and concentrated using centrifugal filter device 10,000 MCO (Millipore), then stored at −20 °C.

2.4. Protein content

The protein concentration was determined by Bradford protein assay using bovine serum albumin as standard (Bradford, 1976). SDS–PAGE analysis was carried out using a 12% polyacrylamide gel under reducing conditional. After electrophoresis protein was stained with modified coomassie brilliant blue G-250 (Kang, Gho, Suh, & Kang, 2002).

2.5. Zymography of HA lyase

The active enzyme was also detected by means of zymography, one of the electrophoretic techniques that includes HA substrate copolymerised with the polyacrylamide gel. Protein sample (HA lyase) were prepared without denaturing the active enzymes present in the samples. Following electrophoresis, the gel is placed in an enzyme activation buffer which allows the enzymes present in the sample to become active and digest the substrates copolymerised in the gel. The zymogram is subsequently stained and the areas of enzyme activity and digestion become visible. Substrate gel electrophoresis of the crude and purified enzyme was performed according to the method described by Yanagishita and Podyma-Inoue (2008) and Mio, Csāka, Stair, and Stern (2001). SDS-PAGE gels were prepared with the laemmi buffer system (Laemmi, 1970), containing 0.17 mg/ml of HA solution in the separating gel. After electrophoresis, SDS was remove from the gels by washing with

2.5% Triton X-100 (Sigma) for 1 h. The gel was washed with incubation buffer (0.1 M phosphate buffer, 0.1 M NaCl at pH: 6) to remove Triton X-100. The incubation buffer was replaced with new buffer and incubated for a 16–18 h at 37 °C. To visualize regions of hyluronan digestion the gels were stained with 0.5% alcian blue in 20% ethanol/10% acetic acid solutions for 1 h, and then destained in a 20% ethanol/10% acetic acid solutions.

2.6. Activity assays of HA lyase

2.6.1. Colorimetric assay

To determine the HA lyase activity quantitatively, the enzyme solution was incubated with 0.5 mg/ml HA solution in a reaction buffer solution containing a 0.1 M phosphate buffer, 0.1 M NaCl (pH ~ 6.0) and bovine serum albumin (BSA, 0.05 mg/ml) at 37 °C. The degradation products were then determined as N-acetylglucosamine (NAG) equivalents by modified Elson Morgan method (Reissig, Strominger, & Leloir, 1955; Takahashi, Ikegami-Kawai, Okuda, & Suzuki, 2003). The rate of release of unsaturated oligomers was measured as the rate of increase in absorbance at 585 nm, using Kc4 micro plate reader spectrophotometer. The amount of the HA lyase that releases 1 μmol of the unsaturated oligomers produced per minute at 37 °C was considered as one HA lyase enzyme unit.

2.6.2. Turbidity assay

A micro assay modified Dofman method was used to measure the HA lyase activity, dependent upon the turbidity reduction at different pH values (Hunnicutt et al., 1996). A 96-well plates were used, and each plate contains, 25 μL/well of HA (0.3 mg/ml) dissolved in a reaction buffer solution containing a 0.1 M phosphate or formate buffer, 0.1 M NaCl and bovine serum albumin (BSA, 0.05 mg/ml) at 37 °C with different pH values, mixed with 25 μL/well HA lyase enzyme diluted in the same reaction buffer for 30 min in humidified chamber. All samples were assayed in triple and the negative control has no HA lyase enzyme. The reaction was stopped by dilution reaction mixture with 0.1 M acetate buffer (pH ~ 3.75) containing 0.1% BSA, then keep stand at room temperature for 10 min. The optical density at wavelength (λ ~ 600 nm) was measured by means of Kc4 micro plate reader spectrophotometer.

2.7. Effect of pH on the activity of HA lyase

The effect of pH on the activity of HA lyase enzyme was examined at various pH ranges (pH ~ 2.0–8.0) using 0.1 M sodium formate, 0.1 M NaCl buffer (pH ~ 2.0–4.0) and 0.1 M sodium phosphate, 0.1 M NaCl buffer (pH ~ 5.0–8.0) at 37 °C using HA as substrate.

2.8. Effect of temperature on the activity of HA lyase

To investigate the effect of temperature on HA lyase activity, the enzyme activity was measured at various temperatures range from 25 to 65 °C in 0.1 M phosphate, NaCl 0.1 M buffer (pH: 6.0) using HA as substrate.

2.9. Effect of metal ions and surfactants on the activity of HA lyase

The HA lyase activities were investigated towards several metal ions; (Ca (II), Mn (II), Zn (II), Co (II), Cu (II), and Mg (II)) at three different concentrations (10, 50 and 100 mM), and surfactants; ionic (SDS), non-ionic (Triton X-100, Tween-20) at four different mole fractions (0.5, 1, 1.5 and 2%). Before assaying the HA lyase residual activity, the enzyme solution was incubated for 15 min at room temperature with presence of different metal ions and surfactants.

2.10. Determination of kinetic parameters of HA lyase

The kinetic parameters (maximal velocity V_{max}, Michaelis constant K_m) of HA lyase were determined from Michaelis–Menten, Lineweaver–Burk and Hans plots. Enzymatic assay was carried out at 37 °C, employing colorimetric method using various HA concentrations ranging from 0.1 to 1.5 mg/ml in 0.1 M phosphate buffer containing 0.1 M NaCl (pH ~ 6.0).

2.11. Dynamic light scattering measurements

The hydrodynamic diameter (d_H) has been determined by means of DLS using a Zetasizer Nano ZS90 (Malvern Instruments Ltd., UK), employed a 4 mW He–Ne laser with a fixed wavelength λ = 633 nm. Dynamic light scattering (DLS) measurements were performed at affixed scattering angle of 90°; thus, the hydrodynamic diameter obtained was an apparent *z*-averaged hydrodynamic diameter. The instrument is equipped with a thermostatic sample chamber for maintaining the desired temperatures within a temperature range of 2–90 °C. The HA lyase sample solution was prepared by incubating 350 μl of HA lyase protein (0.58 mg/ml) in 50 mM acetate buffer (pH ~ 5.5) at 25 °C for 30 min to reach complete equilibrium. The sample was filtered through Millipore 0.22 μm disposal filters prior to DLS measurement. A bubble-free sample of around 1.5 ml was introduced in a quartz cuvette (QC) sample cell through a syringe. The cell was then sealed airtight with a Teflon-coated screw cap to avoid evaporation at a high temperature, and then the cell is secured in a sample chamber of DLS. The temperature of sample cell was controlled by the proportional integral derivative temperature controller to within ±0.1 °C. The DLS measures the Brownian motion of particles and correlates this to the particle sizes. The diffusion coefficient *D* of the particles is directly related to the decay rate τ_c of the time-dependent correlation function for the light-scattering intensity fluctuations:

$$D = \frac{1}{2\tau_c k^2} \quad (1)$$

In this equation *k* is the wave number of the scattered light, $k = (4\pi n/\lambda)\sin(\theta/2)$, where *n* is the refractive index of the solvent, λ is the wavelength of the incident light in vacuum and θ is the scattering angle. The mean hydrodynamic radius of the particles, d_H, was calculated according to the Stokes–Einstein equation (Eq. (2)) (Ashcroft & Mermin, 1988):

$$d_H = \frac{k_B T}{3\pi\eta D} \quad (2)$$

where k_B is the Boltzmann's constant ($1.3806503 \times 10^{-23}\ m^2\ kg\ s^{-2}\ K^{-1}$), *T* is the absolute temperature in K, η is the viscosity of the sample solution (mPa s), and *D* is the diffusion coefficient ($m^2\ s^{-1}$) of particles. DLS data have been accumulated and analyzed with multifunctional real-time correlator Photocor-FC. DynaLS software was used for polydispersity analysis of DLS data.

2.12. UV-circular dichroism spectra

Circular dichroism (CD) measurements were carried out at 25 °C between 150 and 400 nm (0.2 nm/min) using 1-mm quartz cells in Jasco 720-spectrophotometer (Tokyo, Japan). The cell temperature was controlled to within ±0.1 °C by circulating water via a water bath through a cell jacket. It is important that the sample of protein should be homogeneous and should be freed of highly scattering particles by either centrifugation or passage through a suitable filter (e.g., 0.2 μm), and in order to be able to estimate the secondary structure content of a protein sample from CD, it is essen-

Table 1
Purification of HA lyase.

Step	Volume (ml)[a]	Activity (U/ml)	Protein content (mg/ml)	Specific activity (U/mg)	Yield (%)	Purification fold
Crude protein	5	0.95	5.23	0.18	100	1
IMAC[b]	6	0.98	0.27	3.60	124	20
IEX[c]	1	5.58	0.58	9.62	117	53.4

[a] Volume of the purified fraction.
[b] IMAC: immobilized metal affinity chromatography purification using Histrap FF column.
[c] IEX: ion exchange chromatography purification using AKTA chromatography system.

tial to know the protein concentration accurately Protein samples (native HA lyase (0.58 μg/ml), and denatured HA lyase with GdnHCl and urea at different concentrations 1, 2, and 3 M) were prepared in 0.1 M phosphate buffer containing 0.1 M NaCl (pH 6.0) to a working concentration of 58 μg/ml. The spectra obtained were averages of 3 scans and baseline corrected by subtracting the reference spectrum. The spectra were smoothed via an internal algorithm in the Jasco software package, J-700 for Windows. When CD data are expressed in terms of ellipticity, the *mean residue ellipticity* $[\theta]_{mrw,\lambda}$ at a wavelength λ is quoted in units of deg cm^2 dmol^{-1} and is given by Eq. (3):

$$[\theta]_{mrw,\lambda} = \frac{MRW\theta_\lambda}{10dc} \quad (3)$$

where θ_λ is the observed ellipticity (°), d is the path length (cm) and c is the concentration (in units of g/ml). The protein secondary structure contents were calculated from these far UV-circular dichroism spectra (CD) of native and denatured HA lyase using DICHROWEB soft ware's (Whitmore & Wallace, 2004, 2008).

2.13. UV–visible absorption measurements

For the UV–visible absorption spectra, the protein HA lyase (0.58 mg/ml) solutions were prepared in 0.1 M phosphate buffer, 0.1 M NaCl (pH ~ 6.0) at 25 °C for 30 min to reach complete equilibrium and resuspended in a medium containing 0.1 M sodium phosphate, 0.1 M NaCl, at 1, 2, 3 M GdnHCl and 1, 2, 3 M urea. A V-550 spectrophotometer (JASCO) equipped with 0.5 cm quartz cells was used for the UV–visible absorption experiments.

3. Results and discussions

A PCR product of 1.08 kb was obtained by amplification of the interested gene (hylp). *E. coli* BL21 (DE3) harboring the recombinant plasmid pET30b-hylp was induced with 1 mM IPTG and expression level of hylp was analyzed by 12% SDS-PAGE. Time course of protein expression shows that, the maximum level of expression at 3 h after induction. This level of expression remained almost constant. Compared with the molecular mass of bacterial HA lyases (75–130 kDa) (Abramson, 1973; Akhtar & Bhakuni, 2004; Akhtar, Krishnan, & Bhakuni, 2006; Allen et al., 2004; Arvidson, 1983; Gerlach & Köhler, 1972; Hill, 1976; Ingham, Holland, Gowland, & Cunliffe, 1979; Jedrzejas & Chantalat, 2000; Mishra, Akhtar, & Bhakuni, 2006), the phage HA lyase has a smaller molecular weight. The expression of recombinant HA lyase was present predominately (>90%) in soluble fraction. The calculated molecular mass from the amino acid sequence for hylp including six His residues at the C-terminal is 40.34 kDa in conformity with molecular mass about 40 kDa observed in SDS-PAGE (Fig. 1). It was purified to at least 90% purity based on SDS-PAGE analysis (Fig. 1). As shown in the purification table (Table 1), a single metal chelating affinity purification step (IMAC) resulted in a 20-fold increase in purity and the activity recovery yield of 124%. In the crude protein culture, many inhibitors and undesirable proteins were existed. During, the first purification step, all that undesirable proteins and inhibitors were removed, and the yield of HA lyase was increased to be more than 100%. Whiles, the ion exchange purification (IEX) resulted in a 53.4 fold purity increment and the yield decreased to 117% as shown in Table 1. Zymograhy is known to be a sensitive method for analyzing a hydrolytic enzyme in a protein mixture. Therefore, it was employed in Fig. 1 that the highly sensitive zymogram assay revealed the presence of purified active HA lyase with a diffuse electrophoretic mobility apparently around 40 kDa.

The activities of HA lyase were determined at 37 °C in various buffers with a wide pH range (pH ~ 2–8) using HA as a substrate. It was observed that, the purified HA lyase was active over a small pH range (pH ~ 4–7), with maximal activity at pH ~ 6.0 and pH ~ 5.0 for both colorimetric and turbidity methods, respectively. In acidic medium, HA lyase loses most of its activity (pH ~ 3.0), whereas a considerable activity remained in slightly alkaline medium (pH ~ 8.0), about 20% and 58% relative to the maximal activity measured using colorimetric and turbidity assay methods, respec-

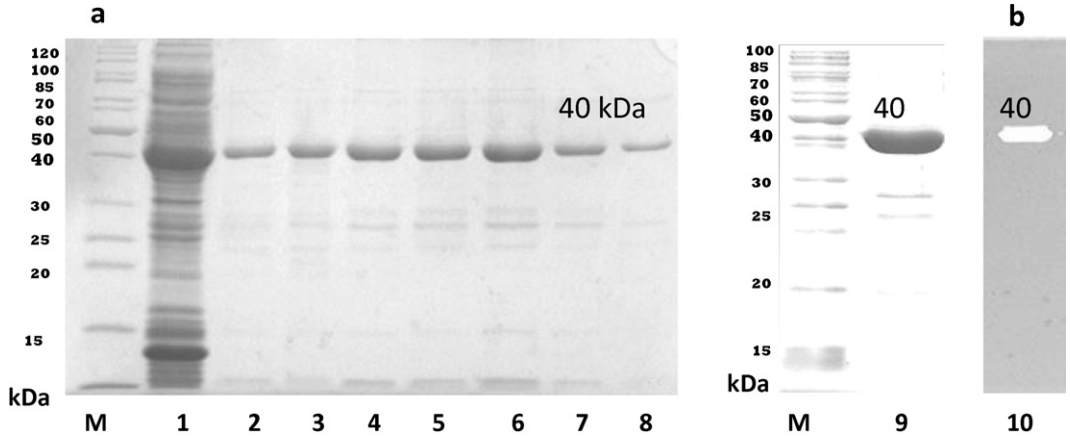

Fig. 1. (a) SDS-PAGE analysis of recombionant HA lyase. Lane M: molecular mass standard protein; Lane 1: Crude protein, Lanes 2–8: Elution fractions resulted from IMAC purification step, Lane 9: Eluted fraction resulted from IEC purification step. (b) Zymogram of an active enzyme with electrophoresis (0.015 μg). Electrophoresis conditions: 125 V, 1 h.

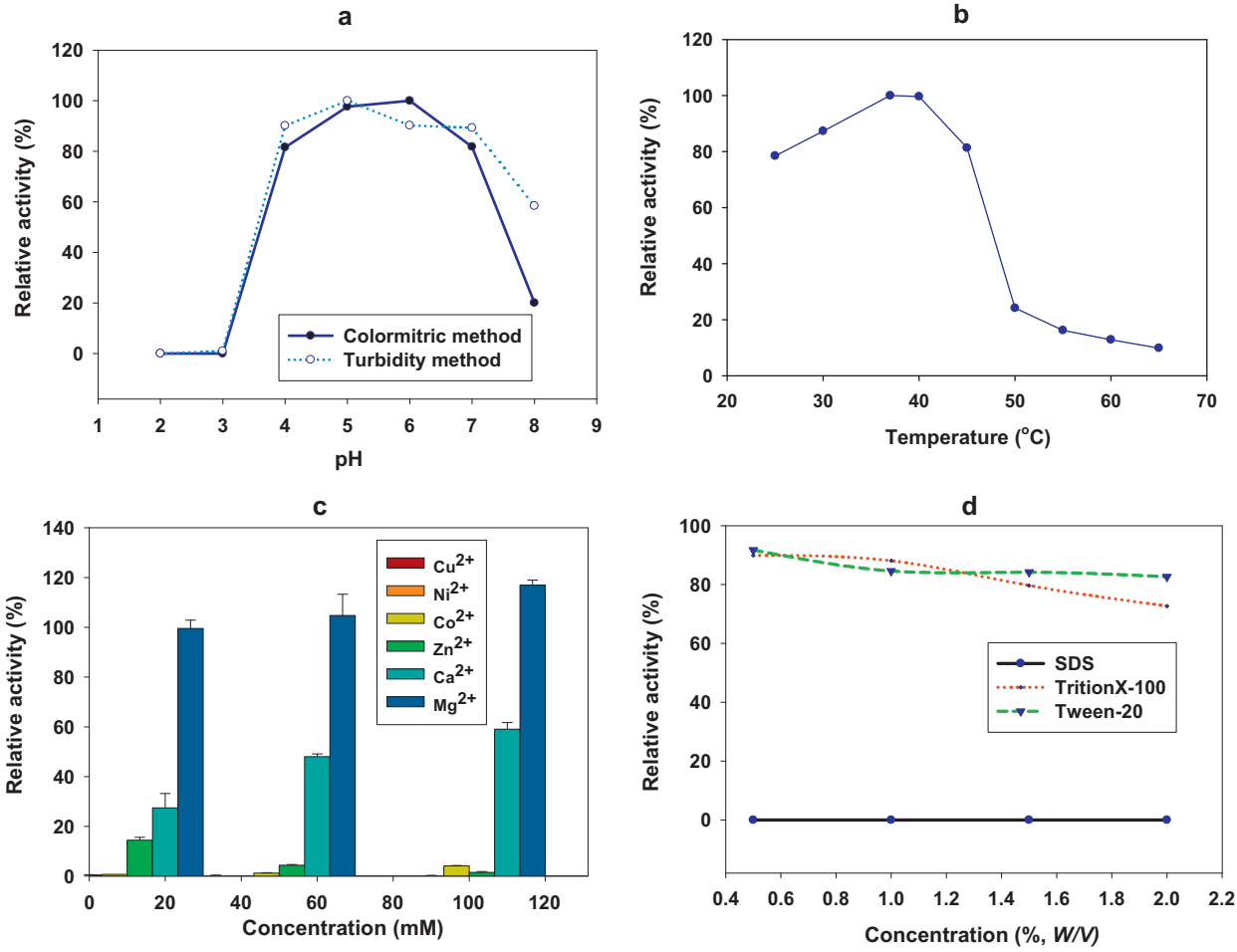

Fig. 2. Effects of (a) pH, (b) temperature, (c) metal ions, and (d) surfactants on the activity of HA lyase.

tively (Fig. 2a). The effect of temperature on the activity of HA lyase was measured in a 0.1 M sodium phosphate buffer, 0.1 M NaCl (pH ~ 6.0). Fig. 2b showed that, the HA lyase gives a maximal activity at 37 °C, and the enzyme had a significant activity in the temperature range 25–45 °C; while over 45 °C, the HA lyase lost more than 70% of its activity. The influence of various metal ions (Ca (II), Ni (II), Zn (II), Co (II), Cu (II), and Mg (II)) and surfactants (ionic (SDS), non-ionic (triton X-100, Tween 20)) on HA lyase activity was investigated at different concentrations under optimum conditions. Among the metal ions studied, Mg (II) metal ion, at concentrations of 10, 50 and 100 mM, stimulated the activity of the HA lyase enzyme by almost 100, 105, and 120%, respectively. However, the metal ion Ca (II) caused a decrease of enzyme activity by 40%, 50%, and 70% at 100 mM, 50 mM, and 10 mM, respectively. In other words, by increasing the Ca (II) concentration, the HA lyase enzyme could be somehow retained its activity. Also, Zn (II) metal ion at the same concentrations (100 mM, 50 mM, and 10 mM) led to reduce of enzyme activity by approximately 98%, 95%, and 85%. Cu (II), Ni (II), and Co (II) metal ions inhibits the HA lyase enzyme activity by almost 99%. This suggested that the metal ions (Ca (II), Ni (II), Zn (II), Co (II), Cu (II)) caused a direct inhibition of the catalytic site of lyase enzyme. The explanation for these various effects (Fig. 2c) lies in the alteration of the enzyme conformation, in which enzymes can be modulated by interaction of metal ions with amino acid residues involved in their active sites. Such interactions can either increase (positive modulation) or decrease (negative modulation) of the enzyme's catalytic activity (Bataillon, Cardinali, Castillon, & Duchiron, 2000; Breccia, Sineriz, Baigori, Castro, & Hatti-Kaul, 1998; Cesar & Mrsa, 1996; Ghanem, Yusef, & Mahrouse, 2000). The experimental results shown in Fig. 2d indicate that non-ionic surfactants (Tween 20 and Triton X-100) inhibit the HA lyase enzyme activity by almost 10–20% at various concentrations. However, the HA lyase enzyme showed no activity in the presence of any concentrations of ionic detergent (SDS). The inhibitory effect of the ionic detergent (SDS) is reasonable because the electrostatic charge of SDS will change the protein tertiary structure to a greater extent, caused a great inhibition on the enzyme activity.

For further understanding the degradation of HA by HA lyase, the substrate kinetic parameters; maximum velocity (V_{max}) and Michaelis constant (K_m) were estimated from a series of reaction rates (V_0) measured at different substrate concentrations (Fig. 3a and b), The experimental data were fitted according to Michaelis–Menten equation by nonlinear regression sigma plot version 10 resulted in values of V_{max} = 0.20 μmol ml^{-1} min^{-1} and K_m = 0.44 mg/ml. To estimate the values of K_m and V_{max} the experimental results were plotted according to the Lineweaver–Burk double reciprocal and Hanes–Woolf models, which rearranges the Michaelis–Menten equation (Fersht, 1998). The linear regression analysis of Lineweaver–Burk double reciprocal plot (Fig. 3b) resulted in kinetic values of ~0.20 μmol ml^{-1} min^{-1} and ~0.44 mg/ml for V_{max} and K_m, respectively, which strongly agrees with the results estimated from hyperbolic curve in Fig. 3b. While, fitting the experimental data in Hanes–Woolf plot gives values of V_{max} of about 0.19 μmol ml^{-1} min^{-1} and K_m of 0.40 mg/ml.

Thermal denaturation and thermal aggregation of HA lyase was studied by means of scattering measurements of a solu-

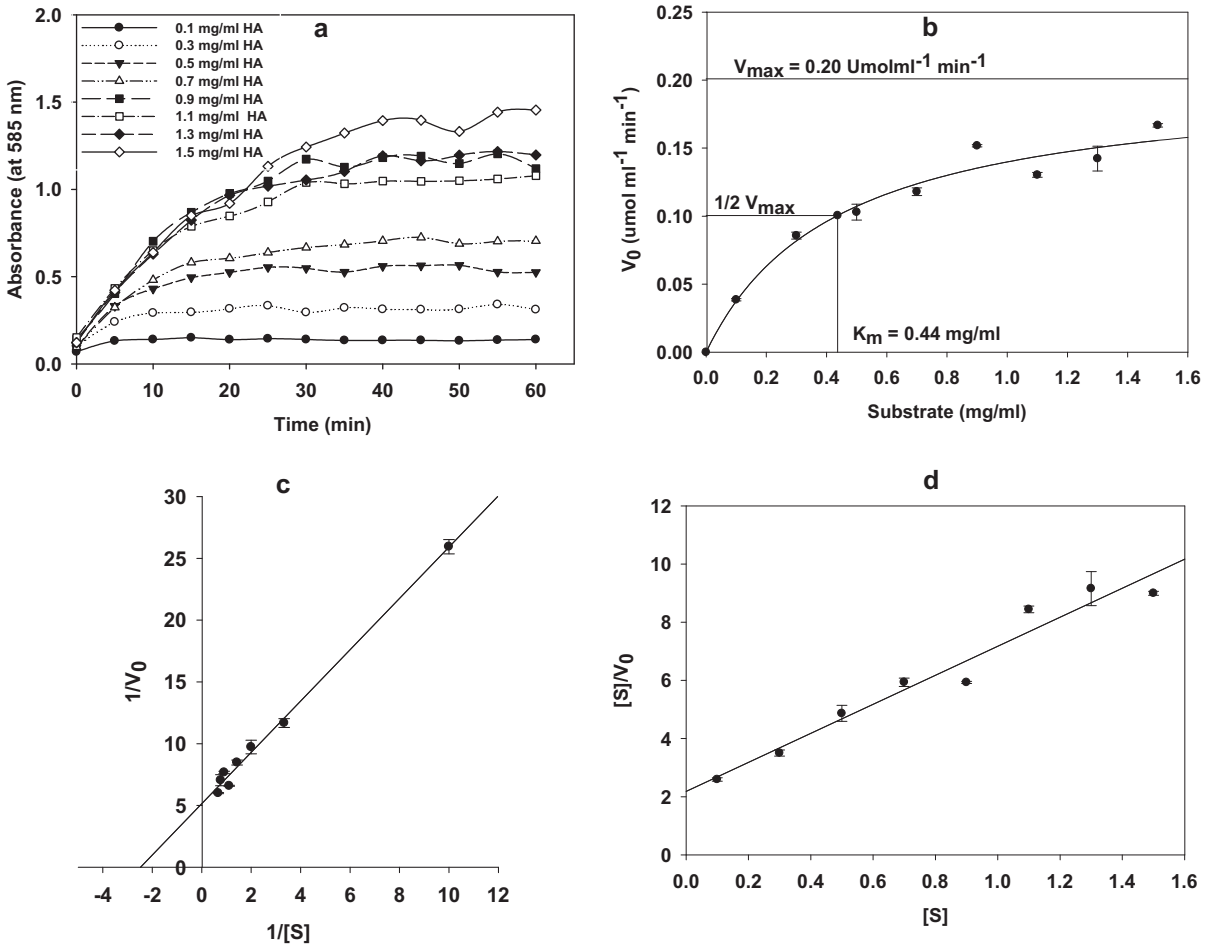

Fig. 3. (a) Time independent kinetics of HA lyase digestion of various HA substrate concentrations, (b) Initial reaction rate, V_0 as a function of HA substrate concentration. The data were fitted to Michaelis–Menten equation by nonlinear regression ($R^2 = 0.9676$). (c) The Lineweaver–Burk double reciprocal plots showing the reaction rate, $1/V_0$ versus HA substrate concentration 1/[S] ($R^2 = 0.9916$), and (d) Hanes–Woolf plot ($R^2 = 0.94986$).

tion containing 350 μl of HA lyase protein (0.58 mg/ml) in 0.1 M phosphate buffer, 0.1 M NaCl (pH ~ 6.0) at various temperatures (25–65 °C). The DLS measurements (Fig. 4a and b) showed that, the first stage of thermal aggregation of HA lyase process is the formation of the start aggregates consisted of denatured protein molecules. Further sticking of the start aggregates and aggregates of higher order proceeds in the regime of what called "diffusion-limited cluster–cluster aggregation" (DLCA) as shown in Fig. 4c (Maloletkina et al., 2010). When this regime is fulfilled, the sticking probability for the colliding particles is equal to unity (Fig. 4d) (Maloletkina et al., 2010). DLS gives direct evidence for the thermal stability of HA lyase evaluated previously in which the enzyme had a significant activity in the temperature range 25–45 °C, then at 46 °C, the enzyme starts to lose most of its activity. Hydrodynamic diameter (d_H) obtained from the DLS spectra of intensity distribution graph (Fig. 5) as a typical size distribution in nanometers of native HA lyase at various temperatures demonstrates the denaturation temperature of the HA lyase enzyme to be 46 °C (T_d).

Far UV-CD experiments were done to investigate the GdnHCl/urea – induced changes in the secondary structure of the HA lyase at increasing GdnHCl/urea concentrations (1, 2, and 3 M). Fig. 6a, summarizes the effect of increasing concentrations of GdnHCl and urea on the CD ellipticity of the HA lyase protein. Interestingly, an initial sharp positive sigmoid curve was observed for the native HA lyase protein at 191.53 nm, inflected at 207.23 nm to a negative broad sigmoidal curve with two peaks at 224.34 nm and 246.52 nm. Interesting results were obtained, in which by increasing the concentrations of GdnHCl denaturant, unordered band wavelength shifts have been observed in both positive and negative molecular CD ellipticity. Also, similar unordered CD ellipticity changes were observed, demonstrating partial unfolding; probably the unfolding of the C and N-terminal portion of the protein molecule. Almost, no changes have been observed on CD molecular ellipticity by increasing the concentrations of urea. Analysis of the far UV-CD spectra through the on line Dichroweb software at http://dichroweb.cryst.bbk.ac.uk/html/home.shtml (Whitmore & Wallace, 2004, 2008) gave consistent results with reasonable goodness-of-fit (Lin, Simossis, Taylor, & Heringa, 2005; Liu, Carbonell, Klein-Seetharaman, & Gopalakrishnan, 2004; Lobley, Whitmore, & Wallace, 2002) using different algorithms for data deconvolution (Table 2). Despite minor differences in the spectra for the two isozymes the calculated secondary structure contents are quite similar (Table 2). The analysis indicates that while helical structure is present, β-structure is the dominant element. Table 2 shows the predicted content of helices and strands in the native and denatured HA lyase, the percent of α-helix and turn structures was decreased by increasing the concentrations of denaturants. While, the β-stranded structures were increased. Similar overall distribution of secondary structure elements has been reported for Glucan lyase from the red alga Gracilariopsis lemaneiformis (Ernst et al., 2005), two GH31 α-glucosidases (Kashiwabara, Azuma, Tsuduki, & Suzuki, 2000; Nichols et al., 2003), and is confirmed by the structure of the α-xylosidase YicI from *E. coli* (Kimura,

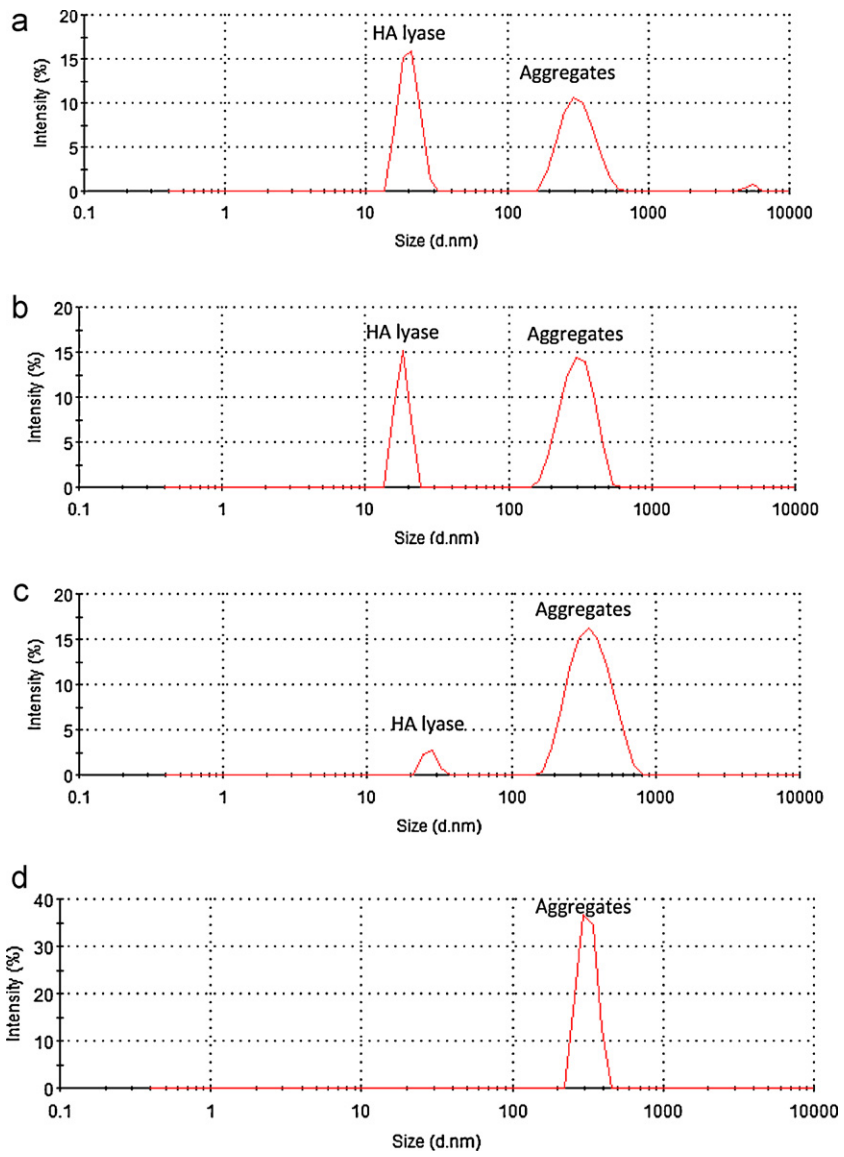

Fig. 4. The distribution of the particles by size registered in the solution of 0.24 mg/ml native HA lyase containing 0.1 mM sodium phosphate buffer, 0.1 M NaCl, pH ~ 6.0 at various temperatures: (a) 25 °C, (b) 37 °C, (c) 47 °C, (d) 49 °C.

Okuyama, Nakai, Mori, & Chiba, 2004; Lovering, Lee, Kim, Withers, & Strynadka, 2005).

It was known that, UV–visible spectroscopy plays an essential role to establish and confirm any alterations or conformational changes done in the protein secondary structure (Tajmir-Riahi, N'Soukpoé-Kossi, & Joly, 2009). The experimental results of UV–visible measurements of HA lyase confirmed the far UV-CD spectral data, that there is a conformational changes in the HA lyase protein secondary structure caused during the denaturation process done by GdnHCl, in which the absorbance measurements of the denaturant HA lyase showed high values than those of the native HA lyase as shown in Fig. 6b. Furthermore, no changes of

Table 2
Secondary structure content calculated from circular dichroism spectra (CD) of native HA lyase and denaturated HA lyase using DICHROWEB computer programs.[a]

Property (%)[b]	Native HA lyase	Denaturated HA lyase					
		GdnHCl			Urea		
Conc.		1M	2M	3M	1M	2M	3M
α-Helix	17.8	13.4	10.2	7.6	17.82	17.73	17.69
B-Strand	31.1	34.2	38.1	40.4	31.17	31.25	31.07
Turns	23.1	23.5	23.4	22.9	23.06	23.13	23.21
Unordered	28	28.9	28.3	29.1	27.95	27.89	28.03
NRMSD[c]	6.3	7.4	5.9	9.1	5.32	4.32	5.01

[a] DICHROWEB: an online server for protein secondary structure analyses from circular dichroism spectroscopic data.
[b] Average of calculated results of SELCON3, CONTINLL, VARSLC & CDSSTR, and K2D models.
[c] Goodness of fit parameter, NRMSD = $\left(\sum(\theta_{exp}-\theta_{calc})^2 \Big| \sum(\theta_{exp})^2\right)^{1/2}$ where θ_{exp} and θ_{calc} are the experimental and calculated molecular ellipticities, respectively.

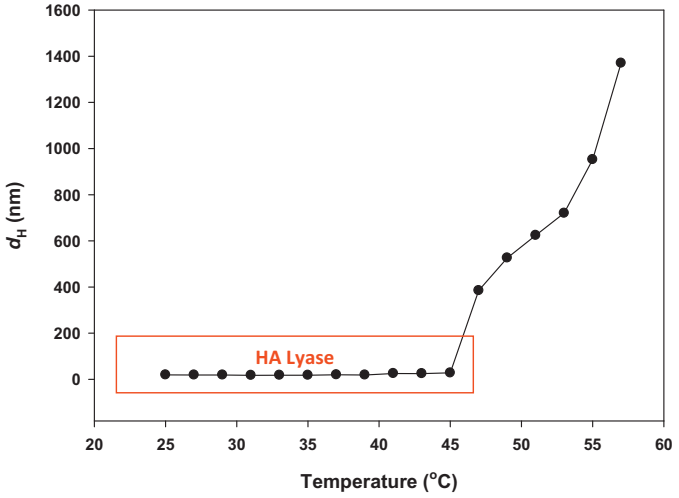

Fig. 5. Hydrodynamic diameter (d_H) obtained from the DLS spectra of intensity distribution graph as a typical size distribution in nanometres of native HA lyase at various temperatures.

the absorbance of HA lyase with or without urea were observed (Fig. 6b). Therefore, the inhibitory effect of urea on the HA lyase does not accompany any alterations in the secondary structure of HA lyase.

Proteins often unfolded under the action of denaturants like GdnHC1 and urea. The intense studies on denaturation of proteins using both theoretical and biophysical method (Dagget & Fersht, 2003; Onuchic & Wolynes, 2004) helps in understanding the protein folding/unfolding mechanism. The unfolding/refolding of a number of proteins under different conditions involves different states that do not appear to be native or completely unfolded (Onuchic & Wolynes, 2004). Different effects of GdnHCl and urea on protein unfolding shows different behavior towards GdnHCl, and urea in terms of different transition processes for these denaturants (Deu & Kirsch, 2007). However, the exact mechanism of action of GdnHCl and urea on proteins is not understood. Urea and guanidine salts have been considered to interact with both the interior hydrophobic areas of protein and the polar peptide portions of the protein chain, which could be considered as partly due to hydrogen bonding (Deu & Kirsch, 2007). These two types of denaturants showed a distinct difference especially in their effects on the α-helical proportion and on the proportion of β-structure in the

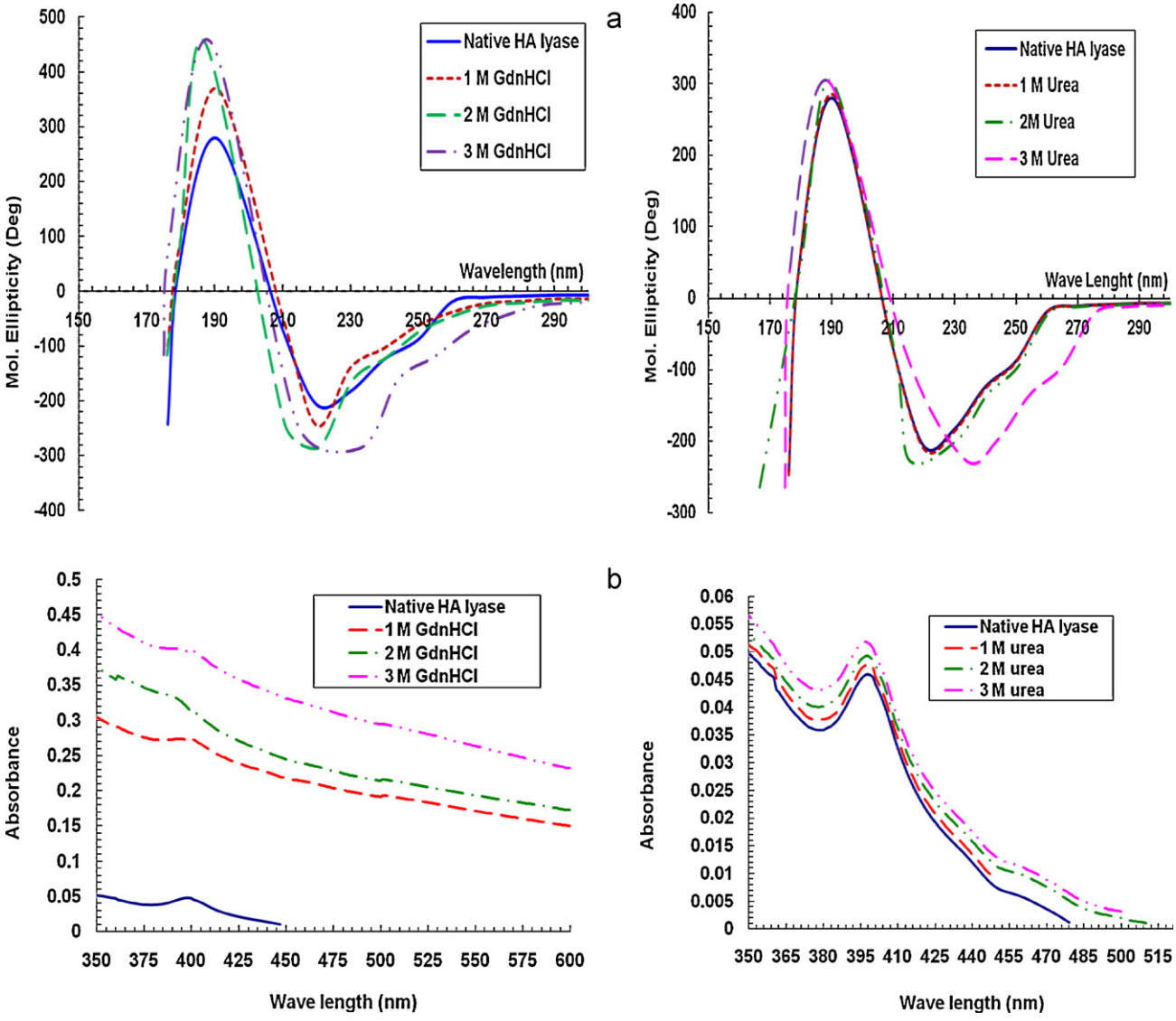

Fig. 6. (a) Far UV-CD spectra, and (b) UV–visible absorption spectra of native and denaturated HA lyase with GdnHCl and Urea at various concentrations.

denaturated HA lyase, as mentioned above. This diverse denaturation effects could be explained based on the mediated denaturation pathways of GdnHCl and urea, in which the urea shows the following mediated denaturation pathway:

$$D \leftrightarrows D^* \leftrightarrows 2U$$

While the mediated denaturation pathway of GdnHCl following this pathway:

$$D \leftrightarrows 2M \leftrightarrows 2M^* \leftrightarrows 2U$$

where D = native dimmer HA lyase, D^* = partially folded dimmer HA lyase, M = folded monomer HA lyase, and U = unfolded HA lyase.

References

Abramson, C. (1973). Staphylococcal hyaluronate lyase. *Contributions to Microbiology and Immunology*, *1*, 376–389.

Akhtar, M. S., & Bhakuni, V. (2004). *Streptococcus pneumoniae* hyaluronate lyase: An overview. *Current Science*, *86*, 285–295.

Akhtar, M. S., Krishnan, M. Y., & Bhakuni, V. (2006). Insights into the mechanism of action of hyaluronate lyase: Role of C-terminal domain and Ca^{2+} in the functional regulation of enzyme. *Journal of Biological Chemistry*, *281*, 28336–28344.

Allen, A. G., Lindsay, H., Seilly, D., Bolitho, S., Peters, S. E., & Maskell, D. J. (2004). Identification and characterisation of hyaluronate lyase from *Streptococcus suis*. *Microbial Pathogenesis*, *36*, 327–335.

Arvidson, S. O. (1983). In C. S. F. Easmon, & C. Adlam (Eds.), *Extracellular enzymes from Staphylococcus aureus Staphylococci and Staphylococcal infections* (pp. 745–808).

Ashcroft, N. W., & Mermin, N. D. (1988). *Solid state physics*. New York: Holt, Rineheart and Winston.

Baker, J. R., Dong, S., & Pritchard, D. G. (2002). The hyaluronan lyase of *Streptococcus pyogenes bacteriophage H4489A*. *Biochemistry Journal*, *365*, 317–322.

Bataillon, M., Cardinali, A. P. N., Castillon, N., & Duchiron, F. (2000). Purification and characterization of a moderately thermostable xylanase from *Bacillus* sp. strain SPS-0. *Enzyme and Microbial Technology*, *26*, 187–192.

Benchetrit, L. C., Gray, E. D., Edstrom, R. D., & Wannamaker, L. W. (1978). Purification and characterization of a hyaluronidase associated with a temperate bacteriophage of group A, type 49 streptococci. *The Journal of Bacteriology*, *134*, 221–228.

Beres, S. B., Sylva, Barbian, K. D., Lei, B., Hoff, J. S., Mammarella, N. D., et al. (2002). Genome sequence of a serotype M3 strain of group A Streptococcus: Phage-encoded toxins, the high-virulence phenotype, and clone emergence. *Proceedings of the National Academy of Sciences of the United States of America*, *99*, 10078–10083.

Berry, A. M., Lock, R. A., Thomas, S. M., Rajan, D. P., Hansman, D., & Paton, J. C. (1994). Cloning and nucleotide sequence of the *Streptococcus pneumoniae* hyaluronidase gene and purification of the enzyme from recombinant *Escherichia coli*. *Infection and Immunity*, *62*, 1101–1108.

Bradford, M. M. (1976). A rapid and sensitive method for the quantitation of microgram quantities of protein utilizing the principle of protein–dye binding. *Analytical Biochemistry*, *72*, 248–254.

Breccia, J. D., Sineriz, F., Baigori, M. D., Castro, G. R., & Hatti-Kaul, R. (1998). Purification and characterization of a thermostable xylanase from *Bacillus amyloliquefaciens*. *Enzyme and Microbial Technology*, *22*, 42–49.

Calvinho, L. F., Almeida, R. A., & Oliver, S. P. (1998). Potential virulence factors of *Streptococcus dysgalactiae* associated with bovine mastitis. *Veterinary Microbiology*, *61*, 93–110.

Cesar, T., & Mrsa, V. (1996). Purification and properties of the xylanase produced by *Thermomyces lanuginosus*. *Enzyme and Microbial Technology*, *19*, 289–296.

Dagget, V., & Fersht, A. (2003). The present view of the mechanism of protein folding. *Nature Reviews*, *4*, 497–502.

Deu, E., & Kirsch, J. F. (2007). The unfolding pathway for Apo *Escherichia coli* aspartate aminotransferase is dependent on the choice of denaturant. *Biochemistry*, *46*, 5810–5818.

El-Safory, N. S., Fazary, A. E., & Lee, C.-K. (2010). Hyaluronidases, a group of glycosidases: Current and future perspectives. *Carbohydrate Polymers*, *81*, 165–181.

Ernst, H. A., Lo Leggio, L., Yu, S., Finnie, C., Svensson, B., & Larsen, S. (2005). Probing the structure of glucan lyases by sequence analysis, circular dichroism and proteolysis. *Biologia – Section Cellular and Molecular Biology*, *60*(SUPPL. 16), 149–159.

Ferretti, J. J., McShan, W. M., Ajdic, D., Savic, G., Lyon, K., Primeaux, C., et al. (2001). Complete genome sequence of an M1 strain of *Streptococcus pyogenes*. *Proceedings of the National Academy of Sciences of the United States of America*, *98*, 4658–4663.

Fersht, A. (1998). *Structure and mechanism in protein science: A guide to enzyme catalysis and protein folding*. San Francisco: Freeman.

Gerlach, D., & Köhler, W. (1972). Hyaluronatlyase von Streptococcus pyogenes. II. Charakterisierung der Hyaluronatlyase (EC 4.2.99.1). *Zentralbl Bakteriol Parasitenkd Infektionskr Hygiene*, *221*, 296–302.

Ghanem, N. B., Yusef, H. H., & Mahrouse, H. K. (2000). Production of *Aspergillus terreus* xylanase in solid-state cultures: Application of the Plackett–Burman experimental design to evaluate nutritional requirements. *Bioresource Technology*, *73*, 113–121.

Gunther, B., Ozegowski, J. H., & Kohler, W. (1996). Occurrence of extracellular hyaluronic acid and hyaluronate lyase in *streptococci* of groups A, B, C, and G. *Zentralblatt fur Bakteriologie*, *285*, 64–73.

Guo, X., Liu, F., Zhu, X., Su, Y., & Ling, p. (2009). Expression of a novel hyaluronidase from *Streptococcus zooepidemicus* in *Escherichia coli* and its application for the preparation of HA oligosaccharides. *Carbohydrate Polymers*, *77*(2), 54–260.

Harrington, D. J., Sutcliffe, I. C., & Chanter, N. (2002). The molecular basis of *Streptococcus equi* infection and disease. *Microbes and Infection*, *4*, 501–510.

Hill, J. (1976). Purification and properties of streptococcal hyaluronate lyase. *Infection and Immunity*, *14*, 726–735.

Homer, K. A., Denbow, L., Whiley, R. A., & Beighton, D. (1993). Chondroitin sulfate depolymerase and hyaluronidase activities of viridans streptococci determined by a sensitive spectrophotometric assay. *Journal of Clinical Microbiology*, *31*, 1648–1651.

Hunnicutt, G. R., Mahan, K., Lathrop, W. F., Ramarao, C. S., Myles, D. G., & Primakoff, P. (1996). Structural relationship of sperm soluble hyaluronidase to the sperm membrane protein PH-20. *Biology of Reproduction*, *54*, 1343–1349.

Hynes, W. L., Dixon, A. R., Walton, S. L., & Aridgides, L. J. (2000). The extracellular hyaluronidase gene (hylA) of Streptococcus pyogenes. *FEMS Microbiology Letters*, *184*, 109–112.

Hynes, W. L., & Ferretti, J. J. (1989). Sequence analysis and expression in *Escherichia coli* of the hyaluronidase gene of *Streptococcus pyogenes* bacteriophage H4489A. *Infection and Immunity*, *57*, 533–539.

Hynes, W. L., Hancock, L., & Ferretti, J. J. (1995). Analysis of a second bacteriophage hyaluronidase gene from *Streptococcus pyogenes*: Evidence for a third hyaluronidase involved in extracellular enzymatic activity. *Infection Immunity*, *63*, 3015–3020.

Hynes, W. L., & Walton, S. L. (2000). Hyaluronidases of Gram-positive bacteria. *FEMS Microbiology Letters*, *183*, 201–207.

Ingham, E., Holland, K. T., Gowland, G., & Cunliffe, W. J. (1979). Purification and partial characterization of hyaluronate lyase (EC 4.2.2.1) from *Propionibacterium acnes*. *Journal of General Microbiology*, *115*, 411–418.

Jedrzejas, M. J., & Chantalat, L. (2000). Structural studies of streptococcus agalactiae hyaluronate lyase. *Acta Crystallographica Section D*, *56*, 460–463.

Kang, D., Gho, Y. S., Suh, M., & Kang, C. (2002). Highly sensitive and fast protein detection with coomassie brilliant blue. In sodium dodecyl sulfate-polyacrylamide gel electrophoresis. *Bulletin of the Korean Chemical Society*, *23*, 1511–1512.

Kashiwabara, S., Azuma, S., Tsuduki, M., & Suzuki, Y. (2000). The primary structure of the subunit in *Bacillus thermoamyloliquefaciens* KP1071 molecular weight 540,000 homohexameric alpha-glucosidase II belonging to the glycosyl hydrolase family 31. *Bioscience, Biotechnology, and Biochemistry*, *64*, 1379–1393.

Kimura, A., Okuyama, M., Nakai, H., Mori, H., & Chiba, S. (2004). Molecular analysis of α-glucosidase (GH-family 31). In S. Janecek (Ed.), *2nd Symposium on the Alpha-Amylase Family – Program and Abstracts* Smolenice Castle, October 3–7, 2004, Lecture L14, ASCO Art & Science, Bratislava, (p. 30).

Kjems, E. (1958). Studies on streptococcal bacteriophages. 2. Adsorption, lysogenization, and one-step growth experiments. *Acta Pathologica et Microbiologica Scandinavica*, *42*, 56–66.

Kostyukova, N. N., Volkova, M. O., Ivanova, V. V., & Kvetnaya, A. S. (1995). A study of pathogenic factors of *Streptococcus pneumoniae* strains causing meningitis. *FEMS Immunology and Medical Microbiology*, *10*, 133–137.

Laemmi, U. K. (1970). Cleavage of structural proteins during the assembly of the head of bacteriophage T4. *Nature*, *227*, 680–685.

Lin, K., Simossis, V. A., Taylor, W. R., & Heringa, J. (2005). A simple and fast secondary structure prediction method using hidden neural networks. *Bioinformatics*, *21*, 152–159.

Linhardt, R. J., Galliher, P. M., & Cooney, C. L. (1986). Polysaccharide lyases. *Applied Biochemistry and Biotechnology*, *12*, 135–176.

Liu, Y., Carbonell, J., Klein-Seetharaman, J., & Gopalakrishnan, V. (2004). Comparison of probabilistic combination methods for protein secondary structure prediction. *Bioinformatics*, *20*, 3099–3107.

Lobley, A., Whitmore, L., & Wallace, B. A. (2002). DICHROWEB: An interactive website for the analysis of protein secondary structure from circular dichroism spectra. *Bioinformatics*, *18*, 211–212.

Lovering, A. L., Lee, S. S., Kim, Y. W., Withers, S. G., & Strynadka, N. C. J. (2005). Mechanistic and structural analysis of a family 31 α-glycosidase and its glycosyl-enzyme intermediate. *Journal of Biological Chemistry*, *280*, 2105–2115.

Lui, G. Y., & Nizet, V. (2004). Extracellular virulence factors of group B Streptococci. *Frontiers in Bioscience*, *9*, 1794–1802.

Maloletkina, O. I., Markossian, K. A., Belousova, L. V., Kleimenov, S. Y., Orlov, V. N., Makeeva, V. F., et al. (2010). Thermal stability and aggregation of creatine kinase from rabbit skeletal muscle. Effect of 2-hydroxypropyl-β-cyclodextrin. *Biophysical Chemistry*, *148*, 121–130.

Marciel, A. M., Kapur, V., & Musser, J. M. (1997). Molecular population genetic analysis of a *Streptococcus pyogenes* bacteriophage-encoded hyaluronidase gene: Recombination contributes to allelic variation. *Microbial Pathogenesis*, *22*, 209–217.

Maxted, W. R. (1952). Enhancement of streptococcal bacteriophage lysis by hyaluronidase. *Nature*, *170*, 1020–1021.

Mio, K., Csãka, A. B., Stair, S. N., & Stern, R. (2001). Detecting hyaluronidase and hyaluronidase inhibitors: Hyaluronan-substrate gel and -inverse substrate gel techniques. *Methods in Molecular Biology*, *171*, 391–397.

Mishra, P., Akhtar, M. S., & Bhakuni, V. (2006). Unusual structural features of the bacteriophage-associated hyaluronate lyase (hylp2). *Journal of Biological Chemistry*, *281*, 7143–7150.

Mishra, P., Kumar, P. R., Ethayathulla, A. S., Singh, N., Sharma, S., Perband, M., et al. (2009). Polysaccharide binding sites in hyaluronate lyase – crystal structures of native phage-encoded hyaluronate lyase and its complexes with ascorbic acid and lactose. *FEBS Journal*, *276*, 3392–3402.

Mukherjee, G., & Banerjee, R. (2006). Effects of temperature, pH and additives on the activity of tannase produced by a co-culture of *Rhizopus oryzae* and *Aspergillus foetidus*. *World Journal of Microbiology and Biotechnology*, *22*, 207–212.

Mukherjee, G., & Banerjee, R. (2007). Some properties of the food processing enzyme tannase produced in a bioreactor by *Aspergillus foetidus*. *Journal of Food Science and Technology*, *44*, 289–292.

Nichols, B. L., Avery, S., Sen, P., Swallow, D. M., Hahn, D., & Sterchi, E. (2003). The maltase-glucoamylase gene: Common ancestry to sucrase-isomaltase with complementary starch digestion activities. *Proceedings of the National Academy of Sciences of the United States of America*, *100*, 1432–1437.

Niemann, H., Birch-Andersen, A., Kjems, E., Mansa, B., & Stirm, S. (1976). Streptococcal bacteriophage 12/12-borne hyaluronidase and its characterization as a lyase (EC 4. 2. 99. 1) by means of streptococcal hyaluronic acid and purified bacteriophage suspensions. *Acta Pathologica et Microbiologica Scandinavica – Section B*, *84*, 145–153.

Onuchic, J. N., & Wolynes, P. G. (2004). Theory of protein folding. *Current Opinion in Structural Biology*, *14*, 70–75.

Polissi, A., Pontiggia, A., Feger, G., Altieri, M., Mottl, H., Ferrari, L., et al. (1998). Large-scale identification of virulence genes from *Streptococcus pneumoniae*. *Infection and Immunity*, *66*, 5620–5629.

Reissig, J. L., Strominger, J. L., & Leloir, L. F. (1955). A modified colorimetric method for the estimation of N-acetylamino sugars. *Journal of Biological Chemistry*, *217*, 959–966.

Schaufuss, P., Sting, R., Schaeg, W., & Blobel, H. (1989). Isolation and characterization of hyaluronidase from *Streptococcus uberis*. *Zentralblatt fur Bakteriologie*, *271*, 46–53.

Smith, N. L., Taylor, E. J., Lindsay, A. M., Charnock, S. J., Turkenburg, J. P., Dodson, E. J., et al. (2005). Structure of a group A streptococcal phage-encoded virulence factor reveals a catalytically active triple-stranded beta-helix. *Proceedings of the National Academy of Sciences of the United States of America*, *102*, 17652–17657.

Smoot, J. C., Barbian, K. D., Gompel, J. J. V., Smoot, L. M., Chaussee, M. S., Sylva, G. L., et al. (2002). Genome sequence and comparative microarray analysis of serotype M18 group A Streptococcus strains associated with acute rheumatic fever outbreaks. *Proceedings of the National Academy of Sciences of the United States of America*, *99*, 4668–4673.

Starrl, C. R., & Engleberg, N. C. (2006). Role of hyaluronidase in subcutaneous spread and growth of group A Streptococcus. *Infection and Immunity*, *74*, 40–48.

Stern, M., & Stern, R. (1992). A collagenous sequence in a prokaryotic hyaluronidase. *Molecular Biology and Evolution*, *9*, 1179–1180.

Tajmir-Riahi, H. A., N'Soukpoé-Kossi, C. N., & Joly, D. (2009). Structural analysis of protein-DNA and protein-RNA interactions by FTIR. UV–visible and CD spectroscopic methods. *Spectroscopy*, *23*, 81–101.

Takahashi, T., Ikegami-Kawai, M., Okuda, R., & Suzuki, K. (2003). A fluorimetric Morgan–Elson assay method for hyaluronidase activity. *Analytical Biochemistry*, *322*, 257–263.

Whitmore, L., & Wallace, B. A. (2004). DICHROWEB, an online server for protein secondary structure analyses from circular dichroism spectroscopic data. *Nucleic Acids Research*, *32*, 668–673.

Whitmore, L., & Wallace, B. A. (2008). Protein secondary structure analyses from circular dichroism spectroscopy: Methods and reference databases. *Biopolymers*, *89*, 392–400.

Yamagata, T., Saito, H., Habuchi, O., & Suzuki, S. (1968). Purification and properties of bacterial chondroitinases and chondrosulfatases. *Journal of Biological Chemistry*, *243*, 1523–1535.

Yanagishita, M., & Podyma-Inoue, K. A. (2008). *Degradation of hyaluronan and its disorder. Experimental glycoscience, part 2, section IX*. (pp. 216–218)